COMPDYN 2023
9th ECCOMAS Thematic Conference on
Computational Methods in Structural Dynamics and Earthquake Engineering
M. J. A. Fritzsche, M. M. Rupp, S. R. Lorenzen, L. Hofmann, L. Birmele, J. Schneider
Athens, Greece, 12-14 June 2023

INVERSE IDENTIFICATION OF CABLE FORCES USING ITS MODAL BEHAVIOR BY DIRECT AND NON-CONTACT VIBRATION MEASUREMENTS

Max J. A. Fritzsche[1], **Maximilian Michael Rupp**[1], **Steven R. Lorenzen**[1], **Lucia Hofmann**[1], **Lia Birmele**[1] **and Jens Schneider**[1]

[1] Technical University of Darmstadt, Institute of Structural Mechanics and Design (ISM+D)
Franziska-Braun-Straße 3, DE-64287 Darmstadt, Germany
{fritzsche,rupp,lorenzen,schneider}@ismd.tu-darmstadt.de
{lucia.hofmann,lia.birmele}@stud.tu-darmstadt.de

Abstract

Cables are essential in civil engineering for constructing slender, lightweight structures with large spans. To ensure serviceability and load-bearing capacity, a monitoring of the cable forces is necessary. Conventional, static methods are not suitable for systems with highly prestressed cables or large cable diameters, so dynamic measurements using the cable's vibration behavior offer an alternative. This study presents laboratory test results on inverse identification of cable forces using eigenmodes and the corresponding frequencies, comparing contact and non-contact dynamic measurement methods. Two methods for determining the cable force will be investigated within this study: (1) the linear theory of vibrating strings neglects internal sag and bending stiffness, and (2) an inverse identification of the cable force for a cable tensioned on both sides, accounting for bending stiffness. Contact based measurement with accelerometers can identify many eigenmodes and frequencies unambiguously and is suitable for simple systems like single span systems. In the conducted investigations, the non-contact measurement with microwave interferometers could only identify up to 4 natural frequencies.
The study also examines the influence of the free vibration length, which, in addition to the bending stiffness of the cable, the fork fitting and utilization, has a significant influence on the determined cable forces. The implications for using different fork fittings and cable cross-sections are discussed. This study offers valuable insights into the challenges and limitations of cable force identification and highlights the importance of choosing the appropriate measurement method based on the design of the cable structure.

Keywords: dynamic measurements, inverse identification, free vibration length, linear theory of vibrating strings, experimental determination of natural frequencies

1 INTRODUCTION

Cables have numerous applications in the construction industry, including as bracing, stiffening elements, and suspension and tensioning cables for suspension bridges and facades. Prestressed cables are often used to avoid failure or too large deformation under compressive stress from external loads. Long-term environmental influences and fatigue can lead to a reduction in prestressing forces, which in turn results in greater deformation that compromises the integrity of the structures or limits their serviceability. Therefore, preventive inspections and periodic checks of cable structures are necessary to detect and address maintenance issues. While permanent monitoring of prestressing forces using installed measuring equipment is an option for some structures, it may not be economically feasible for complete equipment on a cable net facade. Instead, this paper focuses on measurement methods for structure inspections that do not require cables with pre-installed measurement technology, such as static and dynamic measuring methods. Integrated sensors like LoadScan® [1] from Pfeifer Systems GmbH, which measure cable forces with a force measuring unit embedded in clevis joints, will not be considered further.

1.1 Static measurement methods

A conventional method for determining cable forces is through static measurements using a tensioning device. This method involves displacing the tensioning cable at two points relative to a centrally located third point, and the cable force can be determined via the angle or transverse load required to produce a defined sag [2]. Based on Figure 1 and equation (1), the unknown cable force N can be calculated using the angle α and sag s. The cable is then tensioned at two points.

$$N = \frac{s}{2} \cdot \frac{1}{\sin \alpha} \tag{1}$$

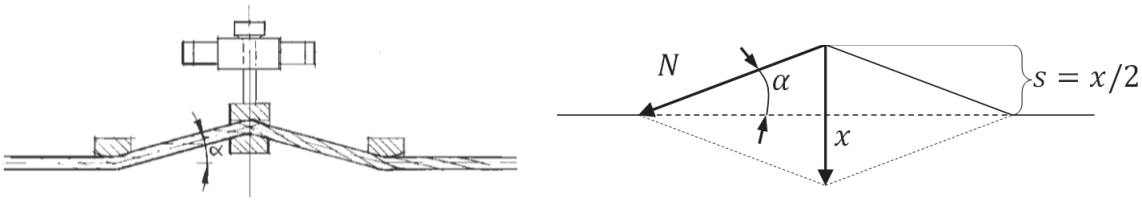

Figure 1: Principle application of a static cable force gauge [2] with illustration of the attachment of the device (left) and evaluation of the cable force according to the cable-tensioning method (right).

A commonly used cable tension measuring device is the PIAB RTM 20 D, manufactured by PIAB Kraftmesstechnik [2]. This device is suitable for cable cross-sections ranging from 6-38 mm diameter, calibrated for four cable ranges using a minicomputer, and provides an accuracy in cable force determination of 2-6% depending on the cable construction. Another widespread device is the CableBull® cable tension sensor from Honigmann [3]. It can be used for material diameters ranging from 1-46 mm but requires one of up to five series with different measuring distances depending on the measuring task. While the manufacturer does not specify a defined accuracy, they claim to have "high accuracy".

1.2 Dynamic measurement methods

An alternative method for measuring dynamic cable force is by determining the cable's natural frequencies. This can be achieved through direct and non-contact vibration measurements, where the linear theory of the vibrating string is utilized to estimate the cable force [4]. However, neglecting the bending stiffness of the cable can lead to inaccurate results, especially for larger

diameters or small span-to-diameter ratios. To account for the bending stiffness, methods such as Morse's approximate solution [5] and Geier and Petz's method [6] have been developed.

To determine the natural frequencies, displacement, velocity or acceleration signals of the cables can be used. Accelerometers are often used due to their versatility, reliability, and low costs, although other sensors such as strain gauges, gyroscopes, or force sensors may be more suitable depending on the application. Direct dynamic measurements on the cable are challenging due to the high effort required to carry out the measurement and ensure accessibility and power supply for wired sensors.

Non-contact measurement methods such as photogrammetry [7], laser scanning [8], and microwave technology [9] are becoming increasingly popular for structural monitoring. However, there are also disadvantages associated with these systems, such as higher signal-to-noise ratio, lower sensitivity, and limited sampling rates for photogrammetry and laser scanning. Consequently, determining higher-order natural frequencies, including harmonics, is challenging during system identification. Our experimental results align with observations from [10] that indicate the first natural frequency can be determined relatively unambiguously, but usually no more than 2-3 harmonics can be identified from the measured signals. Additionally, the evaluation range in this measurement method is carried out in evaluation cells, providing relative displacements in the entire radial resolution cell. The MetaSensing FastGBSAR microwave interferometer used in our study has an evaluation range of approximately 0.75m, which also corresponds to the maximum bandwidth of the waves with an accuracy of ±0.01 mm [11].

2 METHODS

In this section, we will explain the established methods for determining the cable forces based on frequency, with a focus on those applicable to single cables. We will first present the linear theory of the vibrating string, followed by Morse's approximate solution, which considers the bending stiffness of the cable and forms the basis of Geier and Petz's third method. Geier and Petz's method requires at least two natural frequencies to solve the system of linear equations with the two variables, namely the idealized first natural frequency f_{1s} and the related stiffness ξ. Since additional natural frequencies can often be identified, the excess ones can be utilized for optimization using a gradient method [12]. We will not delve into the equations that account for discontinuities in the form of local single masses, as the scope of our research is restricted to single and multi-span cable systems with a constant mass occupancy. Lastly, we investigate the methods that consider the incorporation of individual masses. [13] provides an approach without, and [14] an approach including the consideration of bending stiffness.

2.1 Methods for frequency-based identification of cable forces

2.1.1. Linear theory of the vibrating string

The linear theory of the vibrating string provides the most straightforward approach for determining cable forces. This theory assumes an ideal cable with no bending stiffness that is tightly tensioned. A detailed theory, which accounts for vibrations inside and outside the cable's sheaves, can be found in [4]. According to this theory, Equation (2) can be used to determine the unknown natural frequency f_n as a function of the cable force, where n is the order of the natural frequency f_n, l is the span of the cable, and μ is the mass occupancy.

$$f_n = \frac{\omega}{2 \cdot \pi} = \frac{n}{2} \cdot \sqrt{\frac{N}{\mu \cdot l^2}} \quad with\ n = 1,2, \ldots \tag{2}$$

2.1.2. Method according to Geier and Petz

In [6], several studies on cable-stayed bridges using dynamic measurements of natural frequencies to investigate cable forces concluded that the previously assumed linear relationship between the natural frequencies and their order is only a sufficient approximation for the first 4-5 natural frequencies. These investigations also considered the influence of bending stiffness and bearing conditions of the cable, which can significantly affect the identification of cable forces based on measured natural frequencies. Therefore, Geier modified the linear relationship between the idealized fundamental frequency f_{1s} and the n-th harmonic f_{ns} as a function of cable normal force N and mass occupancy μ, described by equation (3), by developing an approximate solution based on the approximate solution according to Morse [6] for a beam clamped on both sides.

$$f_{ns} = \frac{n}{2 \cdot l} \cdot \sqrt{\frac{N}{\mu}} \tag{3}$$

By additionally introducing the associated stiffness ξ according to equation (4) and inserting it into the Morse nutrient solution, equation (3) simplifies to equation (5):

$$\xi = L \cdot \sqrt{\frac{N}{EI}} \tag{4}$$

$$f_n = n \cdot f_{1s} \cdot \left[1 + \frac{2}{\xi} + \left(4 + \frac{n^2 \cdot \pi^2}{2}\right) \cdot \frac{1}{\xi^2}\right] \tag{5}$$

With the two unknowns f_{1s} and ξ there is a pair of values that can be solved from a number of at least two measured natural frequencies f_n and their corresponding order n. The solution can be done with a gradient method like the Gauss-Newton method [12]. In [17], the method was applied to numerous inclined cables and concluded that the method can reliably determine the cable force with an accuracy of ± 1% when solved with usually 10 to 15 identified natural frequencies. In [6], the method was applied with 10 natural frequencies at a fundamental frequency of the cables of about 3 Hz. It was confirmed that in addition to the natural frequency, the bending stiffness, the bearing conditions and the cable sag must also be taken into account in order to be able to achieve an accuracy of ± 1%.

Since own investigations for smaller spans especially for measurements with the microwave interferometer used in this study often could not identify more than 5 natural frequencies unambiguously, the Levenberg-Marquardt method as explained in [18] was applied as an alternative to the Gauss-Newton method, which due to its robustness requires less natural frequencies to solve in order to achieve the same accuracy in the inverse force identification(cf. Section 3.3).

2.1.3. Approaches with additional consideration of single masses

The approach for additional consideration of single masses of a wire according to [13] is given in equation (6) and the approach with consideration of bending stiffness given in [14] is shown in equation (7), where m_i defines the mass and x_i the Position of all single masses i across the cable.

$$N = \frac{2 \cdot l}{n^2 \cdot \pi^2} \cdot \left[4 \cdot \pi^2 \cdot f_n^2 \cdot \left(\frac{\mu \cdot l}{2} + \sum m_i \cdot \sin^2\left(\frac{n \cdot \pi \cdot x_i}{l}\right)\right) - \frac{n^4 \cdot \pi^4}{2 \cdot l^3} \cdot EI\right] \tag{6}$$

$$N = 2 \cdot \pi^2 \cdot f_1^2 \cdot \left(2 \cdot \mu \cdot \frac{l^2}{\pi^2} + m \cdot \sum \sqrt{x_i \cdot (l - x_i)}\right) \tag{7}$$

2.2 Measurements

2.2.1. Experimental setup

Two dynamic measurement methods were conducted to test the applicability of cable force identification on the test setup shown in Figure 3. The response of an open spiral cable was measured by a microwave interferometer and seismic acceleration sensors that were compared to a load cell as a reference value. The cable was horizontally tensioned with solid steel brackets bolted to an underlying steel beam. The cable is of PG20 type from Pfeifer with a nominal diameter of 14.1 mm and a tensile force of 109 kN [19].

The cable is secured on both ends using fork fitting type 980 and bolt connections with bending-resistant vane plates that are welded onto head plates. The fork cable ends are arranged to allow for free oscillation from top to bottom, which is where most of the excitation and measurements occur. A load cell is attached to the right support between the steel angle as bearing and the head plate to provide a reference value for the cable forces identified via the natural frequencies (cf. Figure 3). To prevent the increase in free vibration length caused by not fixing the head plate to the steel angle, steel profiles were bolted to the substrate and a clamp was used to press against the substructure from above. The background is covered with paperboard to prevent the interference of moving objects with the evaluation of the relative displacement of the microwave interferometer.

The system response is measured using 8 3D acceleration sensors of type TLD356A17 from PCB Piezotronics, with a measuring range of ±10 g and a sensitivity of 500 mV/g [20]. Figure 4 shows the positions of the accelerometers (labeled 1 to 8) and also indicates the locations of the trihedral (square) radar reflectors labeled A to D that were mounted during some measurements. These radar reflectors have orthogonal surfaces and improve the measurement signals of the microwave interferometer compared to measuring the displacement of the cable's pure cross-section [21]. The self-made radar reflectors were 3D printed and covered with stainless steel blanks. Two sizes of radar reflectors were used to investigate the influence of their individual masses (227 g for the small and 290 g for the large) and the reflector edge lengths (6.5 cm and 9.5 cm) on the cable vibration and measurement signals of the microwave interferometer. Figure 5 shows the smaller reflectors arranged eccentrically in relation to the cable axis in the vertical direction on the left, and the larger reflectors arranged concentrically on the right. The orientation of the microwave interferometer in relation to the point of origin (fork joint, left support) is shown in the images in Figure 6 and with the specified coordinates in Table 1. Figure 7 shows an example of the position of the microwave interferometer in plain view with representation of the resolution cells.

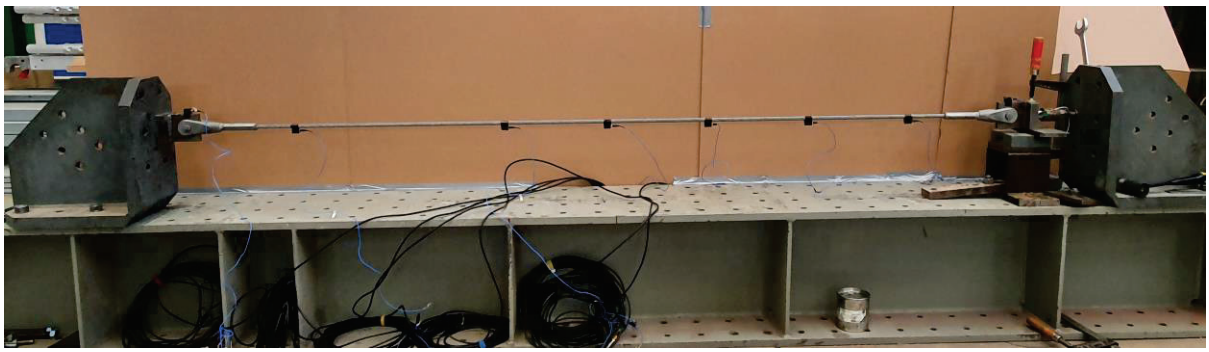

Figure 2: Side view of the test setup.

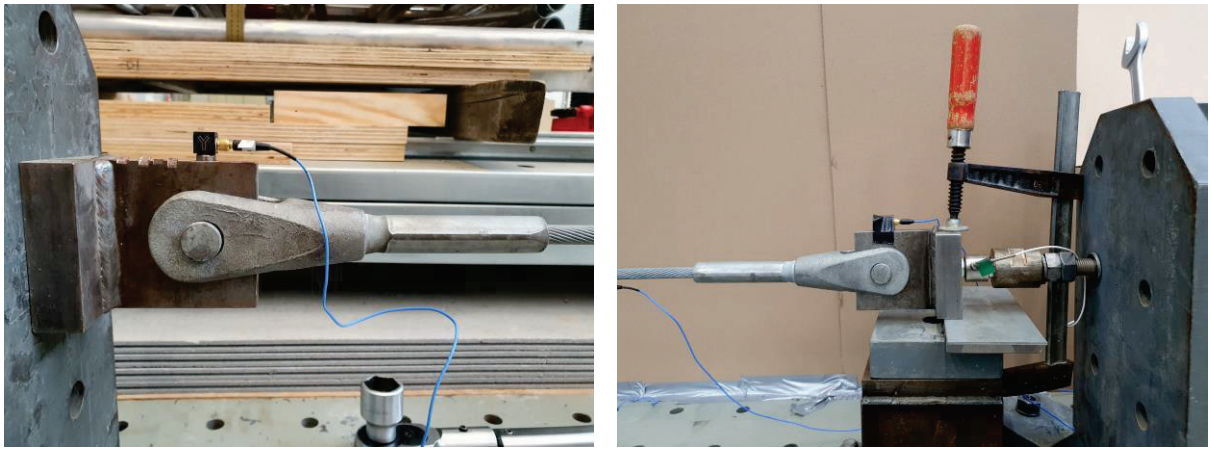

Figure 3: Details of the left and right support.

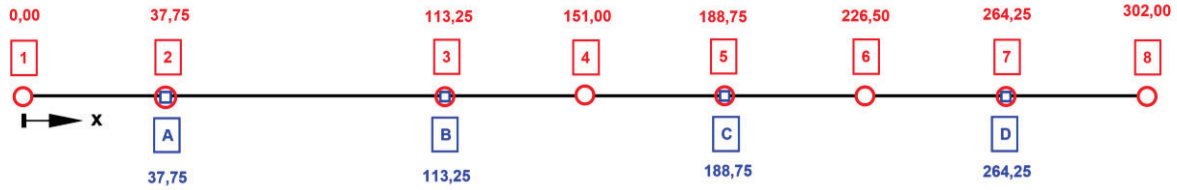

Figure 4: Position of accelerometers {1:8} and optional reflectors {A:D} in cm in relation to the joint in the fork fitting on the left support.

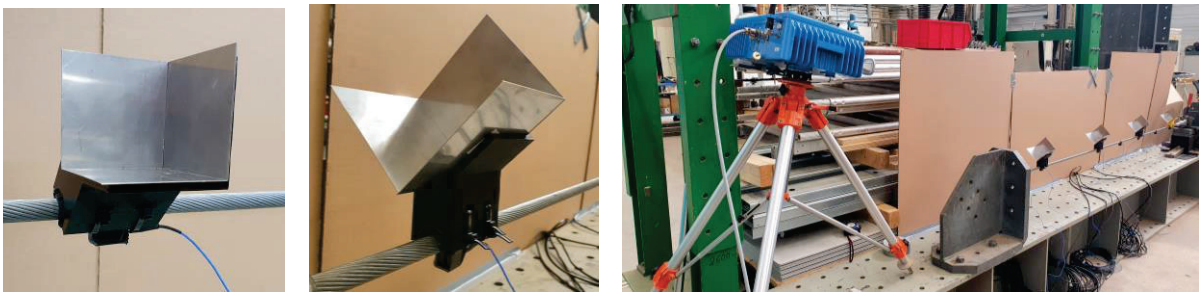

Figure 5: Illustration of the experimental setup with the microwave interferometer positioned at position 3 according to Table 1 with centrally arranged reflectors (left: small reflectors, eccentric; center: large reflectors, centric; right: illustration of experimental setup with 4 reflectors).

Position	X [m]	Y [m]	Z [m]	Inclination [°]
1	-1.32	-0.95	0.00	≈ 0
2	-1.26	-0.92	0.60	≈ 15
3	-1.13	0.00	0.59	≈ 13

Table 1: Coordinates and inclination of the microwave interferometer with respect to the cable axis measured from the left support (clevis pin).

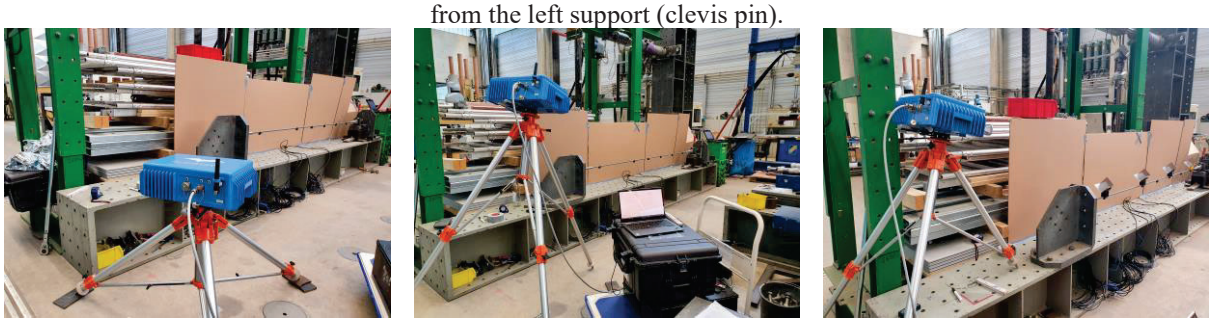

Figure 6: Illustration of the experimental setup with the microwave interferometer positioned according to the orientation given in Table 1 (left: Pos. 1; center: Pos. 2; right: Pos. 3).

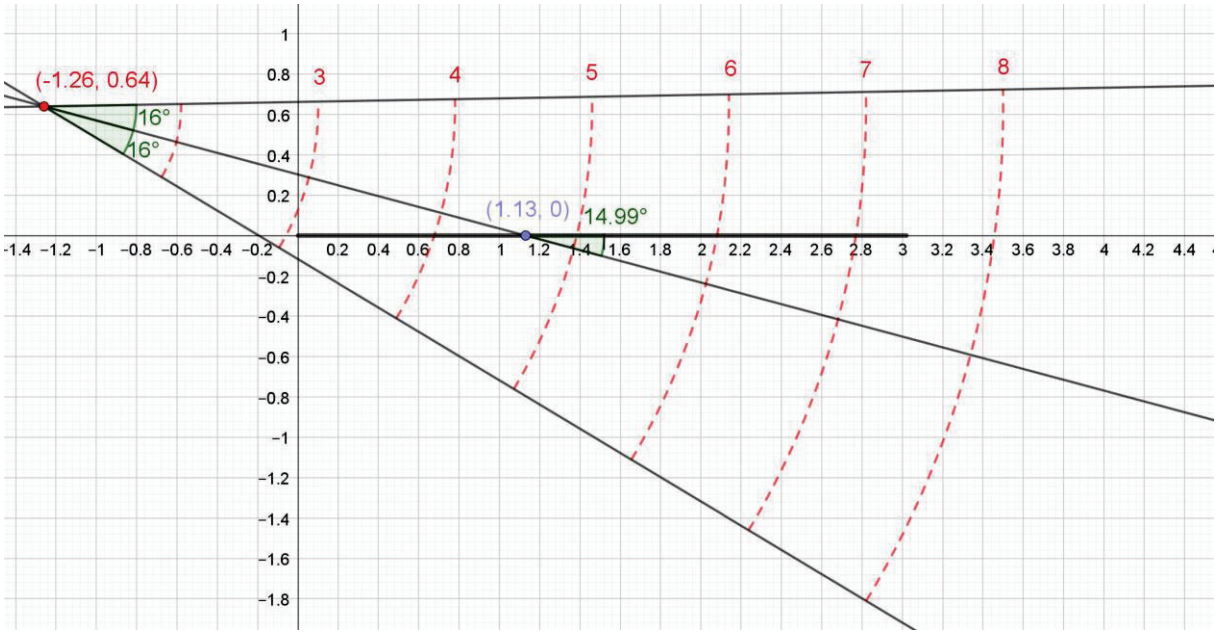

Figure 7: View of position 2 of the microwave interferometer showing the resolution cells $\boldsymbol{i} = \{1{:}8\}$.

2.2.2. Experimental procedure

The experiments were conducted under varying conditions with different test setups involving the use of small and large radar reflectors. Table 2 displays the varied parameters that were employed in the measurement protocol, resulting in a total of 108 recordings with different permutations. For each of the three positions of the microwave interferometer measurements, the target tension forces of 10, 20, 30, and 40 kN were applied, which correspond to utilization rates ranging from 9.2 to 36.7 % concerning the limiting tension force of 109 kN. Higher utilization rates were not possible due to the operating limit of the load cell, which allows a maximum load of 45 kN.

The measurement signal for each of the utilization rates was obtained once without and with small and large radar reflectors, and differentiated between vertical, horizontal, and mixed excitation using an impulse hammer on the cable.

Position	Force in kN	Reflector	Excitation
➢ 1	➢ 10 ($\eta = 0.092$)	➢ none	➢ vertical
➢ 2	➢ 20 ($\eta = 0.183$)	➢ small one	➢ horizontal
➢ 3	➢ 30 ($\eta = 0.275$)	➢ big one	➢ mixed
	➢ 40 ($\eta = 0.367$)		

Table 2: Variable parameters in microwave interferometer measurements.

The acceleration sensors, impulse hammer for forced excitation, and the preload force of the force sensor were measured time-synchronously using a QuantumX MX840B measuring amplifier from Hottinger Brüel & Kjaer GmbH at a sampling rate of 4,800 Hz. The microwave interferometer FastGBSAR from MetaSensing has a resolution cell size of 0.75 m for the bandwidth of approximately 200 MHz, and a sampling rate of 3,787.8788 Hz specified in the program, which results from the wave properties and device configurations. Since the two measuring systems are not synchronized with each other in terms of time, each measurement is first initiated at the measuring amplifier via the Catman® software with a duration of 210 s. Then, the measurement is conducted on a second computer using the Catman® software.

Subsequently, a 180 s measurement is initiated on a second computer using the FastGBSAR controller software, and excitation is applied to record the excitation in both measuring systems over a period of 3 minutes. To achieve a defined pre-tensioning force without effort at the beginning of each measurement, the bar, which is locked with a lock nut on the back of the steel angle, is tightened before each measurement. Subsequently, it was waited until the cable force adjusted to an almost constant value. Then, if necessary, the cable, which is increasingly tensioned flatter with increasing pre-tension, is supported by filler plates and tensioned with the screw clamp. The small normal force from the cable's dead weight at the beginning of the measurement is disregarded due to its short cable length.

3 RESULTS

3.1 Raw measurement data

Experimental results are presented in Figure 8, which shows an example of the measured preload force of the force sensor (left) and the measured acceleration for each sensor (right). In this example, acceleration data of sensor no. 6 with vertical orientation is shown for a measurement with 10 kN preload force and vertical excitation without reflectors. The preload force curve remains nearly constant over time. The time point of the non-periodic force excitation with an impulse hammer is easily recognizable from the large deflection and subsequent free vibration of the cable in the sensor signals. The signals are unambiguous and can be analyzed to study the dynamic system response by filtering the relevant frequency ranges.

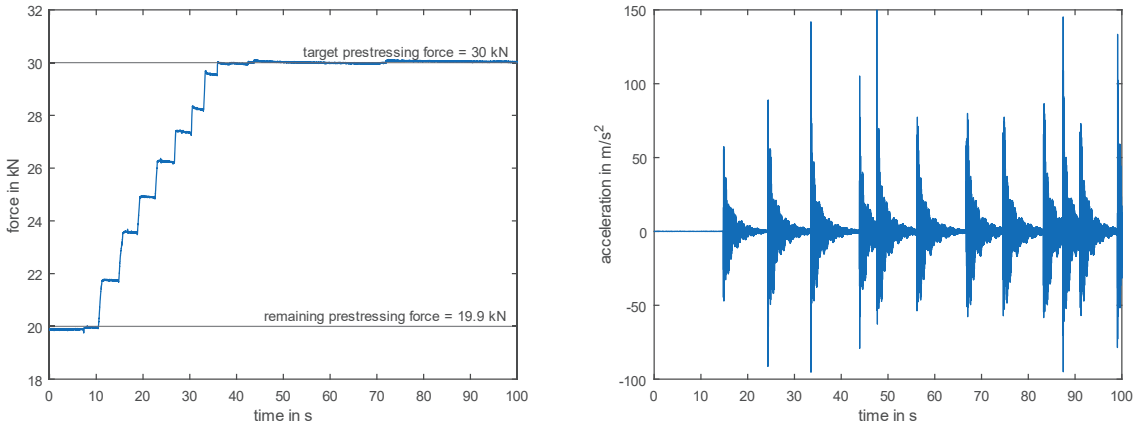

Figure 8: Measurement res ult of the load cell when prestressing force from 30 to 40 kN (left) and representation of the acceleration sensor data from sensor 6 in the local Z direction (right).

The microwave interferometer results were inconclusive. Resolution cells 3-5 did not yield useful measurement results due to low signal noise ratios (SNR). Therefore, Figure 9 only shows the relative displacements for cells 6 - 8 recorded by the measuring instrument. Since resolution cells 6 and 8 displayed jumps with subsequent plateaus and could not be corrected through post-processing, they were not suitable for further evaluation. Hence, Figure 10 shows only the measured displacement values for resolution cell 7, which appears plausible despite the very high noise level.

In the following, we will focus solely on the evaluation of the results obtained from evaluation cell 7, based on the same observations and measurements of other system configurations and prestressing forces. Despite the displacement amplitude being less than 1 mm and the uncertainty regarding whether it was accurate or caused by a defect in the measuring device, we

will proceed with our analysis, since the subsequent analysis of the measurement results will focus on the frequency analysis of the signals, rather than the amplitude of the displacement.

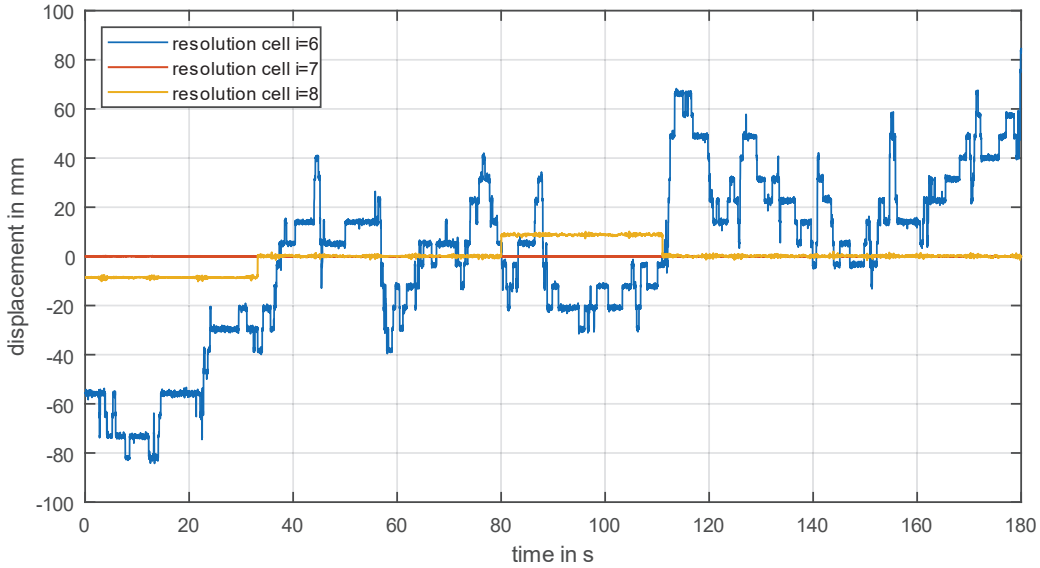

Figure 9: Time-displacement curves for resolution cells 6 to 8 for a measurement without reflector.

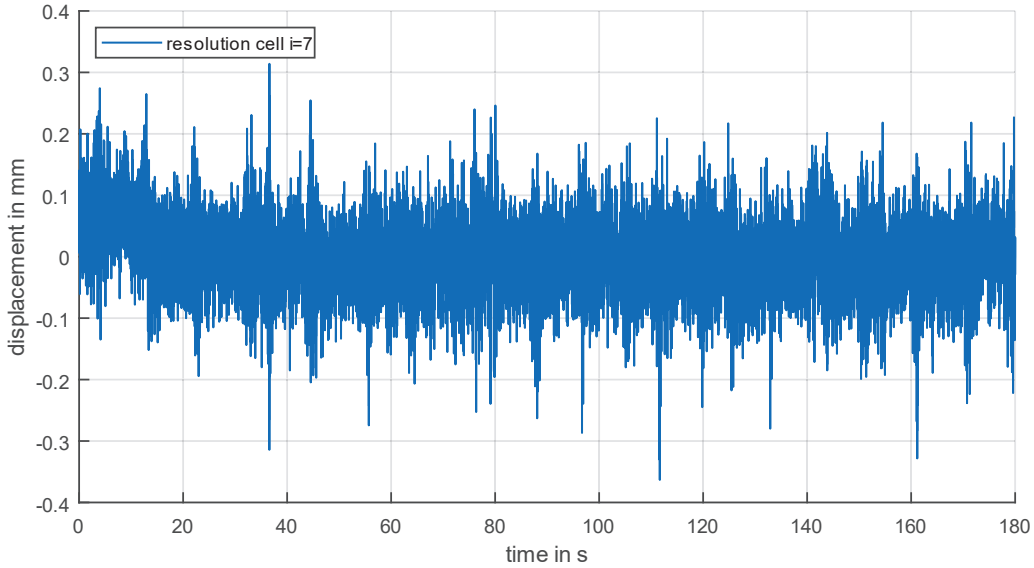

Figure 10: Time-displacement plot for resolution cells 7 without reflector.

3.2 Frequency analysis of the data of both measuring systems

In order to analyze the system response of the measured acceleration sensors and microwave interferometer displacements, a Fast Fourier Transformation (FFT) is applied to the raw data. The resulting frequency spectrum is used to identify the natural frequencies of the system response, by locating the peaks in the spectrum using the fft() function in Matlab®. While the measurement signals of the acceleration sensors exhibit numerous natural frequencies, the microwave interferometer signal is often characterized by a high level of noise, making it challenging to identify any frequencies beyond the fundamental one. To improve peak clarity in the FFT, the signal from the microwave interferometer is divided into eight subintervals. A FFT is

then performed for each subinterval to reduce noise, and the first natural frequency is identified by detecting the local extreme value. The phase angle of the (complex) value of the FFT belonging to the first natural frequency is then calculated to enable synchronization of the partial FFTs over the first natural frequencies identified in all partial FFTs. The resulting averaged FFTs, depicted in Figure 11 and Figure 12, reveal up to four natural frequencies. Since a narrow main lobe of the signal is desired, no explicit windowing (rectangular window) is utilized. The leakage effect due to the relatively short observation period of the subintervals is compensated for by averaging the individual FFTs.

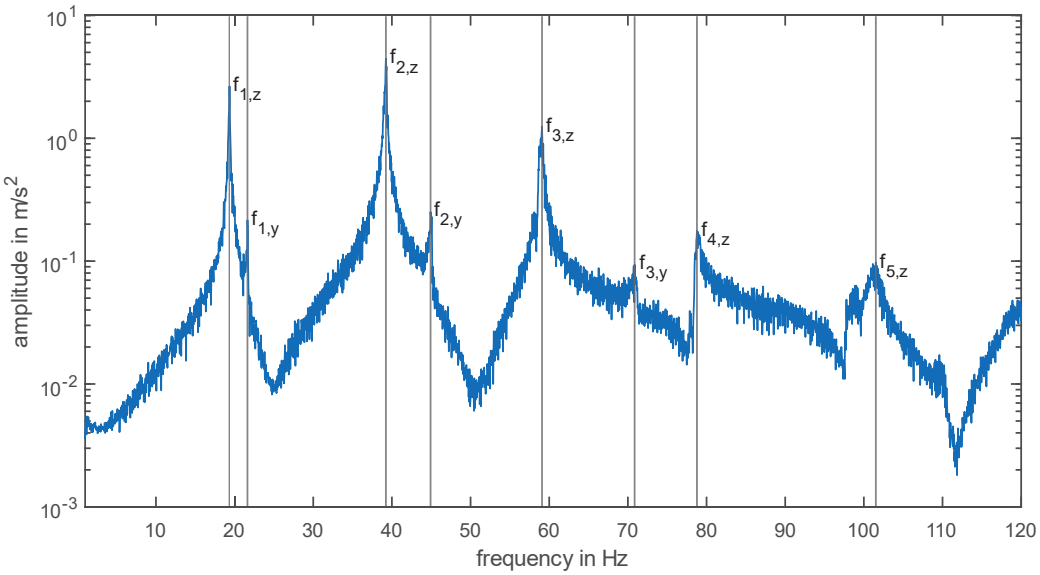

Figure 11: FFT of 8 time intervals for the acceleration data of sensor 6.

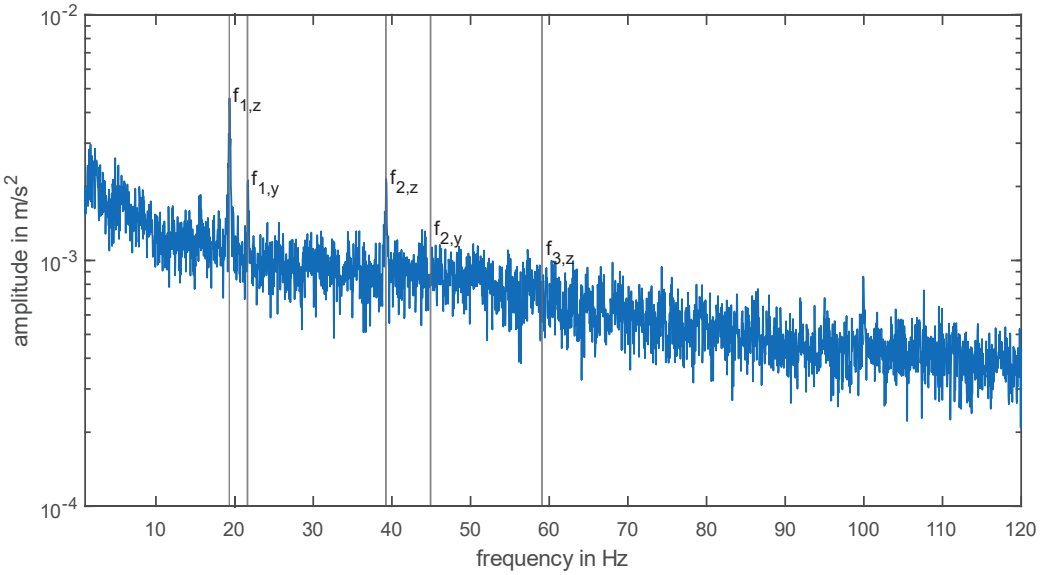

Figure 12: FFT of 8 time intervals for the displacement data from resolution cell 7 for a measurement without radar reflectors.

In brief, the analysis of the frequency of both measurement signals indicates that identification of the fundamental frequency is feasible using FFT for both systems. The acceleration signals exhibit numerous harmonics that can be readily identified without further post-

processing, enabling optimization of the cable force identification through gradient methods. However, the frequency spectra of the microwave interferometer displacements exhibit a significantly higher noise level, making it challenging to identify harmonics without subdividing and analyzing individual partial intervals and subsequently superimposing the partial FFTs. Even with this extensive post-processing of the measured data, typically no more than 2 to 4 natural frequencies can be identified, limiting the optimization of force identification using gradient methods.

3.3 Inverse cable force determination

In this section, the results for cable force identification via natural frequencies are compared with the reference values of the load cell. Not the absolute values, but the relative deviation ΔN of the identified cable force N_{cal} to the reference value of the load cell N_{ref} are determined.

$$\Delta N = \frac{(N_{\mathrm{ref}} - N_{\mathrm{cal}})}{N_{\mathrm{ref}}} \cdot 100\ \% \tag{8}$$

The frequency analysis of the microwave interferometer data identified only the first four natural frequencies. The aim of this study is to investigate the suitability of both methods - direct measurement with acceleration sensors and non-contact measurement using a microwave interferometer - for determining the inverse cable force. Therefore, we will only use the first four natural frequencies in the solution approaches below.

In addition to the identification according to the linear theory of the vibrating string using the fundamental frequency, the influence of the optimization based on including the first four harmonics is also considered using the Levenberg-Marquardt method. For the measurements with radar reflectors, the approaches considering additional concentrated loads according to section 2.1.3 with additional consideration of the bending stiffness are correctly used.

The results in in Figure 13 show that all approaches yield deviations of less than 20 % compared to the reference value of the load cell, with deviations becoming smaller with increasing utilization. The method according to Geier and Petz (cf. 2.1.2) shows the lowest error with a maximum deviation of 10 %, with deviations decreasing rapidly with increasing utilization or pre-stress force, amounting to only about 5 % at the highest utilization of 36.7 %. The results from the back calculation considering concentrated loads due to the radar reflectors show good agreement with the approximation from [14]. For the linear theory of the vibrating string, no improvement can be derived from the consideration of several natural frequencies compared to the calculation using only the fundamental frequency. Therefore, a calculation based on one frequency is sufficient if this approach is followed. Finally, it is investigated to what extent a modified system length defined as effective cable length l_{eff} can be used to achieve smaller deviations in identified forces, excluding the measurements with radar reflectors. A compensation line function is determined as a function of the prestressing force N (cf. equation (9)) to determine the effective cable length l_{eff}.

Figure 14 shows the measurement results without reflectors compared to the system length l for comparison of the results adjusted with l. It can be seen that the deviations from the reference value can be significantly reduced and are below 5 % regardless of the process.

$$l_{eff} = \frac{N}{3kN/cm} + 0.92 \cdot l \tag{9}$$

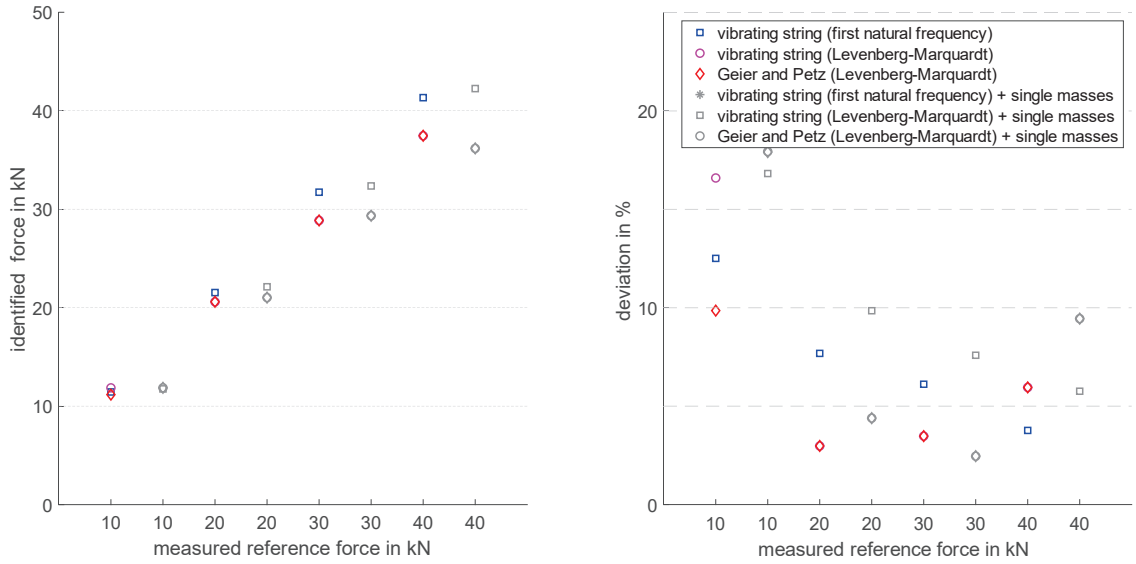

Figure 13: Identified forces and deviations for measurements considering the individual masses from the reflectors for the measurements from position 3.

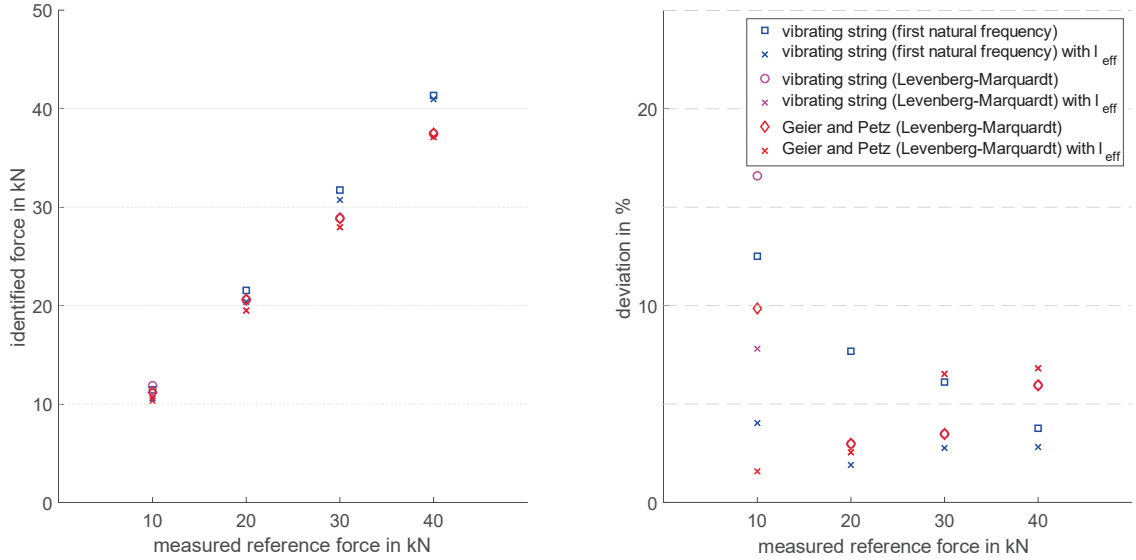

Figure 14: Identified forces and deviations with experimentally determined effective oscillation length $\boldsymbol{l_{eff}}$ for position 3 for measurements without reflectors.

Finally, we utilized the effective cable length as the system length and applied the linear theory of the oscillating string to identify the cable forces based on the first natural frequency. This frequency was determined using both measurement methods. Figure 15 shows the results obtained for the four utilization rates and all measurements without the radar reflector. The outcomes reveal an average deviation of less than 5%, which was further reduced to less than 3% with higher and more realistic utilization rates exceeding 20%. However, the largest standard deviation, observed in the case of the highest utilization with a pre-stressing force of 40kN, was 0.92%.

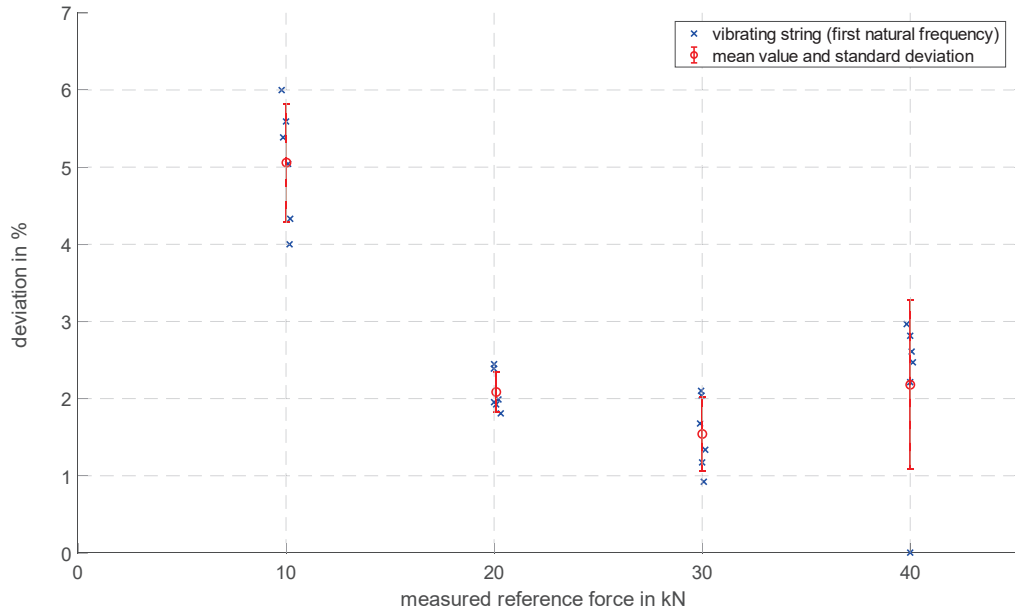

Figure 15: Deviations of the identified cable forces from the first natural frequency according to string theory considering a reduced oscillation length for measurements without reflectors.

4 CONCLUSION

In this investigation, two measurement concepts were evaluated for identifying the natural frequencies of a horizontally tensioned single-span cable. The first approach used acceleration sensors, while the second utilized ground-based microwave interferometers for deformation monitoring. The identified natural frequencies were then used to investigate the validity of equations available in the literature for frequency-based identification of the cable forces.

The use of acceleration sensors was found to be effective for system identification and could identify a large number of harmonics. However, difficulties with accessibility and interaction of secondary supporting or facade elements could arise in real structures. On the other hand, using the microwave interferometer for measurement was much simpler in terms of device placement. However, documenting the position of the resolution cells after the measurement required significant effort to ensure accurate orientation with respect to the measurement object. Strongly oscillating substructures could also have an influence on the measuring results, making them useless. In terms of accuracy, no significant difference was found between the two measuring systems, and both were suitable to identify the fundamental frequency of a cable. Despite the ease of using the microwave interferometer for measurement, documenting and analysing the friction data required a significantly more complex effort. Therefore, the relatively lower additional cost of installing acceleration sensors, even in positions that may require elevating platforms for access, seems justifiable compared to the documentation and evaluation efforts associated with the microwave interferometer.

The results of the cable force identification showed deviations from the reference value of the load cell between 10-20%, which became smaller with increasing utilization of the respective prestressing. Modifying the system length to the effective cable length of the system reduced the deviation to less than 5% using the linear theory of the vibrating string with fundamental frequency approach. However, investigations on other cable cross sections, spans and utilization rates showed that this approach is not generally valid and varies for each system configuration.

To summarize the findings regarding cable force identification, while modifying the effective cable length can improve accuracy, this approach is not universally applicable and varies depending on the specific cable configuration. Therefore, further investigations are necessary to account for influences such as bending stiffness, span length, prestressing force, and cable end formation. Additionally, the use of a microwave interferometer is not suitable for measuring small cable cross-sections and systems with adjoining substructures, unlike for cable-stayed bridges.

REFERENCES

[1] "Permanent monitoring Temporäre Lastkontrolle Permanente Überwachung Accuracy Genauigkeit Universeller Einsatz." PFEIFER Seil- und Hebetechnik GmbH, Memmingen, p. 2, 2023. [Online]. Available: https://fabritecstructures.com/wp-content/uploads/2020/06/2020-Loadscan-brochure.pdf

[2] "PIAB RTM 20 D mit Beschreibung," vol. 1, no. 12. Matthias Nier PIAB, Haldensleben, pp. 0–12. [Online]. Available: http://www.piab-deutschland.de/wp-content/uploads/brosch/RTM_Bedienungsanleitung.pdf

[3] "Honigmann Industrielle Elektronik GmbH - Seilspannungssensor CableBull®.pdf." Honigmann GmbH, Gevelsberg, p. 4, 2023. [Online]. Available: https://honigmann.com/i437/Seilkraftmesser-Seilspannungsmesser-Seilspannungsmessgerät-CableBull.html?lang=1

[4] H. M. Irvine and T. K. Caughey, "The linear theory of free vibrations of a suspended cable," *Proc. R. Soc. London. A. Math. Phys. Sci.*, vol. 341, no. 1626, pp. 299–315, 1974, doi: 10.1098/rspa.1974.0189.

[5] P. M. Morse and K. U. Ingard, *Theoretical acoustics*. Princeton university press, 1986.

[6] R. Geier and J. Petz, "Kraftbestimmung in Schrägseilen durch dynamische Messungen," *Beton- und Stahlbetonbau*, vol. 99, no. 12, pp. 985–991, 2004, doi: 10.1002/best.200490285.

[7] D. Erdenebat and D. Waldmann, "Application of the DAD method for damage localisation on an existing bridge structure using close-range UAV photogrammetry," *Eng. Struct.*, vol. 218, no. March, p. 110727, 2020, doi: 10.1016/j.engstruct.2020.110727.

[8] F. Schill and A. Eichhorn, "Deformation Monitoring of Railway Bridges with a Profile Laser Scanner," *ZfV-Zeitschrift für Geodäsie, Geoinf. und Landmanagement*, vol. 2, pp. 109–118, 2019, doi: 10.12902/zfv-0248-2018.

[9] A. Firus, J. Schneider, M. Becker, J. J. Pullamthara, and G. Grunert, "Microwave interferometry measurements for railway-specific applications," *COMPDYN 2017 - Proc. 6th Int. Conf. Comput. Methods Struct. Dyn. Earthq. Eng.*, vol. 2, no. January, pp. 2705–2718, 2017, doi: 10.7712/120117.5600.17334.

[10] W. Zhao, G. Zhang, and J. Zhang, "Cable force estimation of a long-span cable-stayed bridge with microwave interferometric radar," *Comput. Civ. Infrastruct. Eng.*, vol. 35, no. 12, pp. 1419–1433, 2020, doi: 10.1111/mice.12557.

[11] "FASTGBSAR FAST Ground-Based Synthetic Aperture Radar FastGBSAR is a family of Ku-band ground based radars for deformation monitoring designed to work

FastGBSAR-S." MetaSensing BV, Noordwijk (Netherlands), p. 2, 2017. [Online]. Available: https://metasensing.com/wp-content/uploads/2022/09/MetaSensing-FastGBSAR-general.pdf

[12] M. Stadler, E. Penka, and K. Zilch, "Ermittlung der freien Schwingungslänge zur Bestimmung der Vorspannkraft externer Bandspannglieder durch dynamische Messungen," *Bauingenieur*, vol. 1, no. 82, 2007, [Online]. Available: https://structurae.net/en/literature/journal-article/ermittlung-der-freien-schwingungslange-zur-bestimmung-der-vorspannkraft-externer-bandspannglieder-durch-dynamische-messungen

[13] U. Kuhlmann, "Bauen mit Seilen," *Stahlbau Kal.*, pp. 689–755, 2000.

[14] R. Kempter, *Längskraftmessung von Zugstäben durch Messung der Eigenfrequenz*. München: Hochschule München, 2009.

[15] F. Lottersberger, *Untersuchung einer schienengebundenen Seilbahnfahrt*. Graz (Österreich): Technische Universität Graz, 2010.

[16] M. Schlaich, A. Bögle, and A. Bleicher, *Brückenbau II - Seile*. Berlin: Technische Universität Berlin, 2011.

[17] R. Geier, *Brückendynamik - Schwingungsuntersuchungen von Schrägseilen*. Norderstedt: BoD – Books on Demand, 2004.

[18] W. Dahmen, *Numerik für Ingenieure und Naturwissenschaftler*. 2006. doi: 10.1007/3-540-29883-5.

[19] P. S. Hebetechnik, "PFEIFER-Zugglieder." PFEIFER Seil- und Hebetechnik GmbH, Memmingen, 2015. [Online]. Available: https://www.pfeifer.info/out/assets/PFEIFER_TENSION-MEMBERS_BROCHURE_EN.PDF

[20] P. C. B. Piezotronics, "Model 352C04 General purpose , ceramic shear ICP ® accel ., 10 mV / g , 0 . 5 to 10k Hz , 10-32 Installation and Operating Manual," 2007.

[21] S. Rödelsperger, *Real-time Processing of Ground Based Synthetic Aperture Radar (GB-SAR) Measurements*. 2011. [Online]. Available: http://tuprints.ulb.tu-darmstadt.de/id/eprint/2755